

Electronic Supplementary Information for

Effects of Stereo-regularity on the Single-chain Mechanics of Poly(lactic Acid) and Its Implications on the Physical Properties of the Bulk Materials

Bo Cheng,^{a,c} Lu Qian,^a Hu-jun Qian,^b Zhong-yuan Lu,^b Shuxun Cui^{*,a}

^a Key Lab of Advanced Technologies of Materials, Ministry of Education of China, Southwest Jiaotong University, Chengdu 610031, P. R. China.

^b State Key Laboratory of Supramolecular Structure and Materials, Institute of Theoretical Chemistry, Jilin University, Changchun, 130023, P. R. China.

^c School of Mechanical and Power Engineering, North University of China, Taiyuan 030051, P. R. China.

* Email: cuishuxun@swjtu.edu.cn

Experimental Section:

Materials and Sample Preparation: PLLA and PDLLA samples are all purchased from Shuyuan Biological Science and Technology Co., Ltd. (Jinan, China). The molecular weight (Mn) of PLLA and PDLLA are 260,000 g mol⁻¹ and 280,000 g mol⁻¹, respectively. Deionized (DI) water (>15 MΩ·cm) is used when water is involved. All other chemical reagents are purchased from Sigma and are analytically pure, if not mentioned otherwise. For the sample preparation, the polymer is dissolved into 1,1,2,2-tetrachloroethane (TCE) to different concentrations, i.e., 3, 30, 100 and 1000 μg mL⁻¹. The amino-group modified quartz slide that treated by (3-aminopropyl)-triethoxysilane is prepared according to the literature.¹ About 100 μL of the PLA solution is dropped onto an amino-group modified quartz slide. Then the sample is stored at room temperature until all TCE solvent is evaporated off. Before the force measurements, the same amount of pure TCE solvent will be added onto the sample to regenerate the PLA solution to a concentration same to that for the adsorption. This concentration will be kept during the force measurements (with an error of less than 10%). Thus, the concentration of PLA solution for adsorption can be regarded as the actual concentration of PLA in force measurements.

Force Measurements: All force measurements are performed on a commercial AFM (MFP-3D, Asylum Research, CA) with a V-shaped Si₃N₄ AFM cantilever (MLCT type, Bruker Corp., CA). During the AFM manipulation, data are recorded at the same time and converted to F-E curves subsequently. The spring constant of each AFM cantilever is calibrated by the thermo-excitation method, ranging from 20 to 50 pN nm⁻¹. The stretching velocity applied in this study is 2.0 μm s⁻¹, if not mentioned otherwise. The experimental details of the AFM instrumentation can be found elsewhere.²

Table S1. The comparison of the mechanical and thermal properties between the bulk PLLA and PDLLA materials.^{3,4}

	Configuration	T _g	Tensile strength	Impact resistance
PDLLA	Amorphous	50 °C	40-53 MPa	1.5-2.0 kJ m ⁻²
PLLA	Crystal	55 °C	50-70 MPa	3.0-7.0 kJ m ⁻²

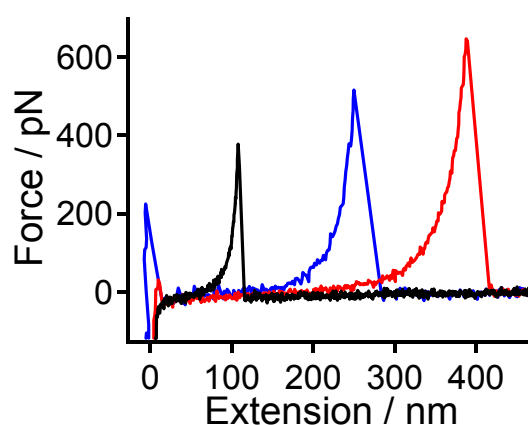


Figure S1. The experimental force curves of PLLA at low concentration obtained in TCE.

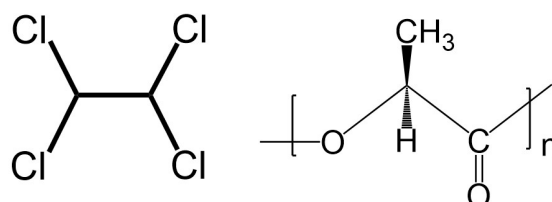


Figure S2. The molecular structures of TCE (left) and PLLA (right).

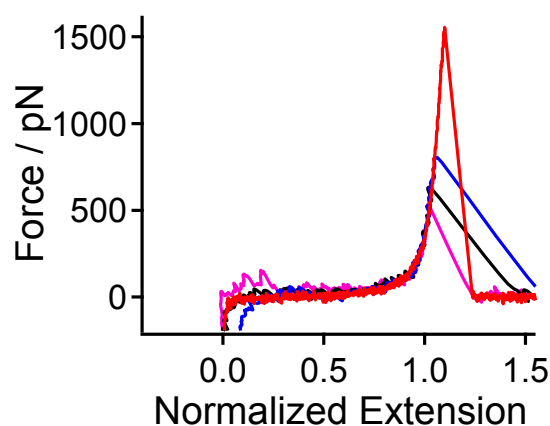


Figure S3. Normalized force curves of PLLA (< 30 μg·mL⁻¹) obtained in octylbenzene.

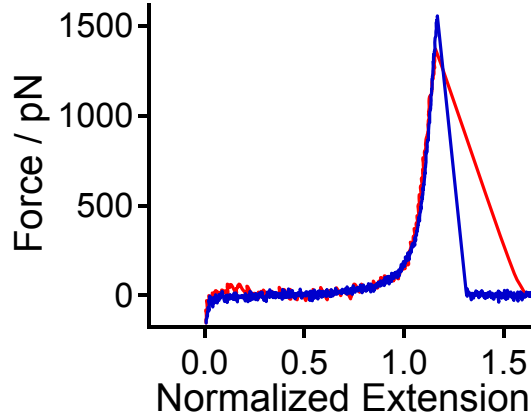


Figure S4. The control experiments of PLLA in octane. The comparison of normalized force curves of PLLA obtained in octane (red line) and octylbenzene (blue line).

The details of QM-FRC model

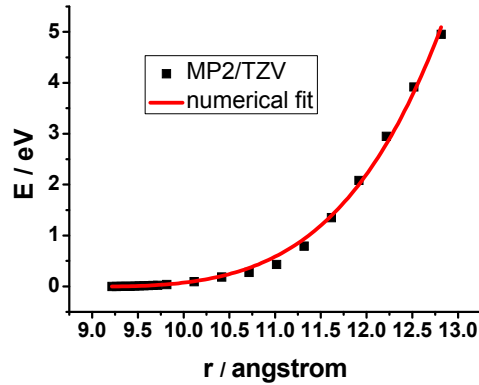


Figure S5. The energies of stretched configurations at fixed distances between two ending oxygen and carbon atoms of single unit of PLLA calculated at the MP2/TZV//B3LYP/TZV dual-level of theory. Solid line denotes the polynomial fit with Equation S1.

The theoretical single PLA chain enthalpic elasticity from QM calculations at the MP2 level (see Figure S5) can be described by a polynomial expansion, see Equation S1 below.

$$F = \sum_{n=1}^5 \gamma_n (L[F]/L_0 - 1)^n \quad \gamma_1 = 2.71 \text{ nN}, \quad \gamma_2 = 1.03 \text{ nN}, \quad \gamma_3 = -202.83 \text{ nN},$$

$$\gamma_4 = 2612.15 \text{ nN}, \quad \gamma_5 = -4963.28 \text{ nN} \quad \text{Equation S1}$$

In this equation, γ_1 is the linear modulus, and other coefficients are nonlinear modulus that will be important at high forces.

The mathematical expression of the QM-FRC model is shown below:

$$R/L_0 = (L[F]/L_0) \cdot [1 - k_B T / (2F \cdot l_b)] \quad \text{Equation S2}$$

In this equation, F is the external stretching force, R is the end-to-end distance of the polymer chain under F , $L[F]$ is the F dependent contour length of the polymer chain, L_0 is the contour length at $F = 0$, k_B is the Boltzmann constant, T is the absolute temperature, and l_b denotes the length of the rotating unit of the polymer chain.

In the QM-FRC model, F can be obtained with a given value of $L[F]/L_0$ from Equation S1. Thus, there is only one free parameter, l_b , in the model. Then the QM-FRC model fitting curve can be obtained by Equation S2.

The details of the process of QM-FRC fitting

The process is briefly described as follows: during the stretching of single PLLA chain, the end-to-end distance of the chain, R , is enlarged gradually with the increasing F to its contour length. The value of $L[F]/L_0$ will begin to rise from 1 to a maximum value when the polymer bridge is broken. Thus, assuming 2000 pN be to the upper limit of rupture force,⁵ the maximum value of $L[F]/L_0$ can be calculated by Equation S1 to be 1.22. For a given value of l_b , R/L_0 can be obtained with each F in the range of 0-2000 pN by using Equation S1 and S2, which actually generates a QM-FRC model fitting curve for l_b .

The details of QM calculations

All quantum mechanical (QM) calculations are carried out using the GAUSSIAN 09 program. The distance between the two ending oxygen and carbon atoms is fixed at different values in our calculations, while the positions of all other atoms are optimized to minimize the total energy. The calculations are performed at the MP2/TZV//B3LYP/TZV dual-level of theory. Figure S4 presents the energy difference by stretching single PLLA unit at fixed

distances between two ending atoms, taking the unstretched PLLA unit ground state as the energy reference. The solid line in Figure S4 denotes polynomial fit according to

$$E = E_0 - a_0 \sum_{n=2}^4 \gamma_{n-1} (a[E]/a_0 - 1)^n / n \quad \text{Equation S3}$$

where a_0 is the length of the repeating unit at zero force, $a_{[E]}$ is the length at a given extension with energy E . Fitting QM data to Equation S3 gives $\gamma_1 = 2.71$ nN, $\gamma_2 = 1.03$ nN, and $\gamma_3 = -2023$ nN, $\gamma_4 = 2612.15$ nN, $\gamma_5 = -4963.28$ nN. The derivative of this equation leads to the force expression, which is actually measurable experimentally,

$$F = \frac{\partial E}{\partial \alpha} = \sum_{n=1}^3 \gamma_n (\alpha[E] / \alpha_0 - 1)^n \quad \text{Equation S4}$$

where $a_{[F]}$ is the length at the given force, F .

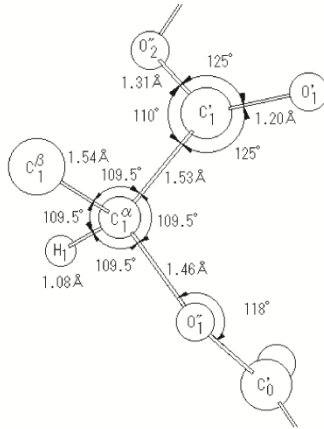


Figure S6. The structural parameters of a single repeating unit of PLA.⁶ The bond length and the bond angle of all bonds in one repeating unit of PLLA are shown.

The details of the choice of the best value of l_b

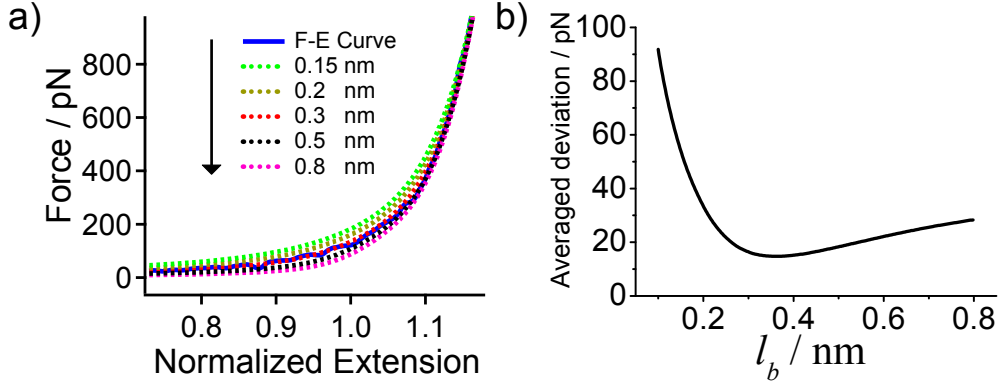


Figure S7. (a) The comparison between the experimental force curve of PLLA obtained in octylbenzene (blue line) and the fitting curves of QM-FRC with different l_b (from 0.15 to 0.8 nm). (b) The averaged force deviation between the experimental force curve and the fitting curves. When l_b is 0.36 nm, the minimum of the averaged force deviation can be reached.

Since l_b is the only free parameter in the model, the choice of the value of l_b is crucial to the fitting performance. As shown in Figure S5a, all the curves are superposed very well in the high force region. This is because that the high force region is mainly dominated by the enthalpic elasticity, which is fixed by the modulus obtained from the QM calculations (Equation S1). However, in the middle force region, there is a marked deviation between the experimental force curve and fitting curves, which is varied with l_b . This is because that the value of l_b is related to the quantities of rotating units in a certain polymer chain: The smaller l_b , the more rotating units in the polymer chain.⁷ Therefore, the entropic elasticity can be affected by the value of l_b : The smaller l_b , the higher entropic elasticity.

To find out the best l_b , we analyze the difference between the experimental curve and the fitting curve with different l_b . In this analysis, we use a formula $\sum_{i=1}^n (|F_{\text{exp}} - F_{\text{fit}}|) / n$ to calculate the average force deviation of the two curves. With a small interval of 0.01 nm, we calculated the differences with each l_b in the range of 0.15 nm to 0.8 nm. As shown in Figure S5b, when l_b is equal to 0.36 nm, the average deviation of F reaches the minimum value, 14.7

pN, which is very close to that of the noise signal (15.4 pN). This result indicates that 0.36 nm is the optimum value of l_b for PLLA in by the QM-FRC model.

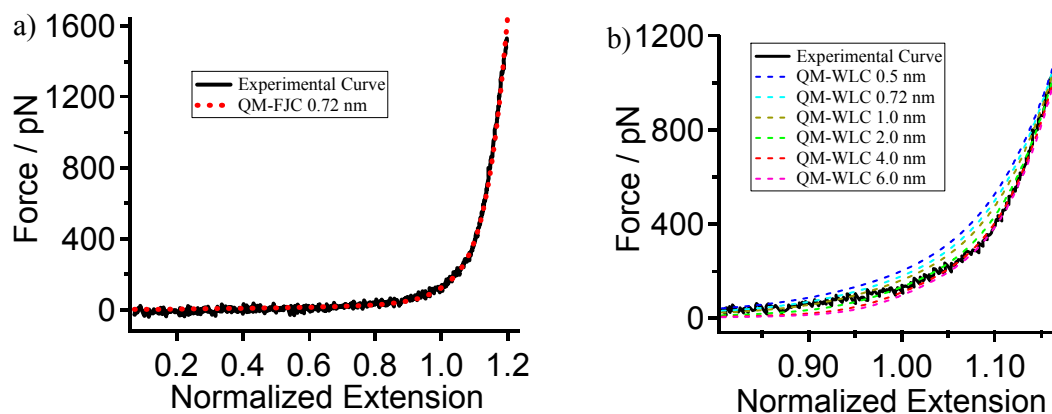


Figure S8. (a) The experimental curve of PLLA at low concentration and the QM-FJC fitting curve with a Kuhn length of 0.72 nm. (b) The comparison of the experimental curve of PLLA at low concentration and the QM-WLC fitting curve with various persistence length from 0.5 to 6.0 nm.

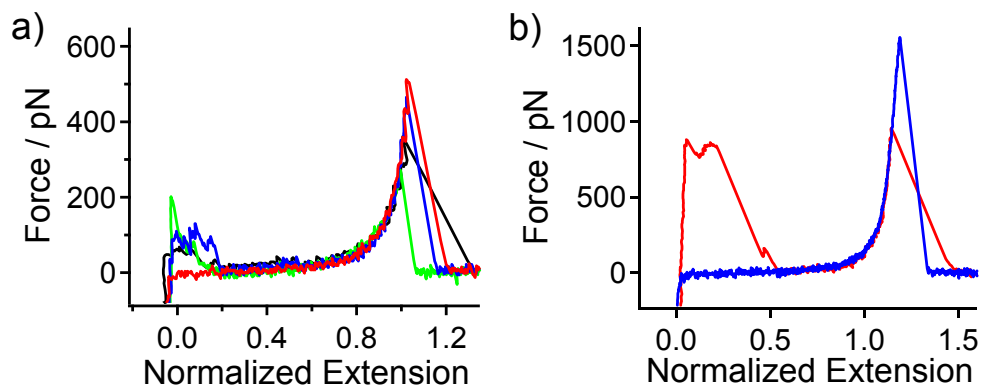


Figure S9. (a) Normalized force curves of PDLLA ($< 30 \mu\text{g}\cdot\text{mL}^{-1}$) obtained in octylbenzene. (b) The comparison of the force curves of PLLA (blue line) and PDLLA (red line) both obtained in octylbenzene (concentration of the starting TCE solution $< 30 \mu\text{g}\cdot\text{mL}^{-1}$).

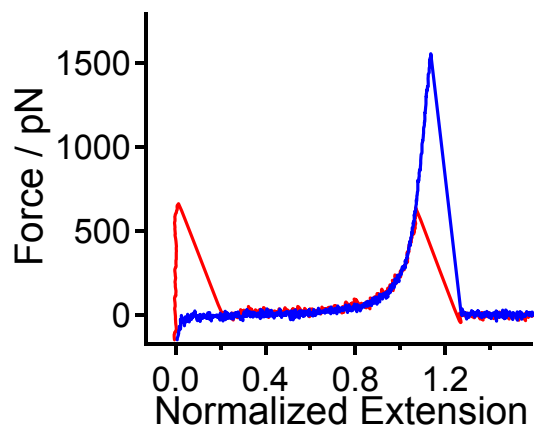


Figure S10. The comparison of the normalized force curves of PLLA ($1000 \mu\text{g}\cdot\text{mL}^{-1}$, red line) obtained in water and the force curve of PLLA obtained in octylbenzene (blue line).

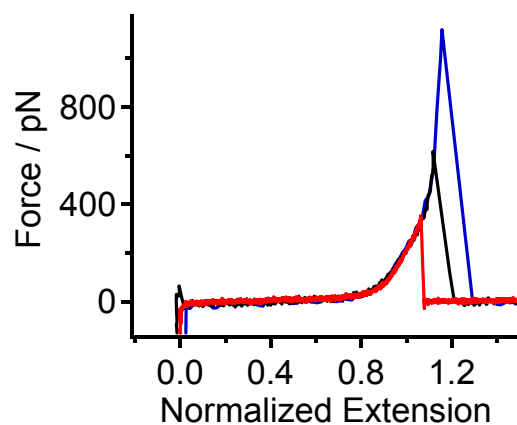


Figure S11. Normalized force curves of PLLA ($1000 \mu\text{g}\cdot\text{mL}^{-1}$) obtained in TCE at different stretching velocities of 0.2 (red line), 2 (black line) and 10 $\mu\text{m}\cdot\text{s}^{-1}$ (blue line), respectively.

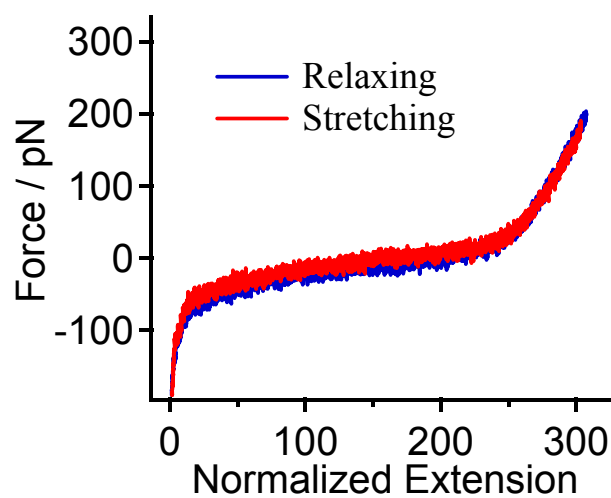


Figure S12. The stretching-relaxing force curves of PLLA obtained in TCE ($1000 \mu\text{g}\cdot\text{mL}^{-1}$).

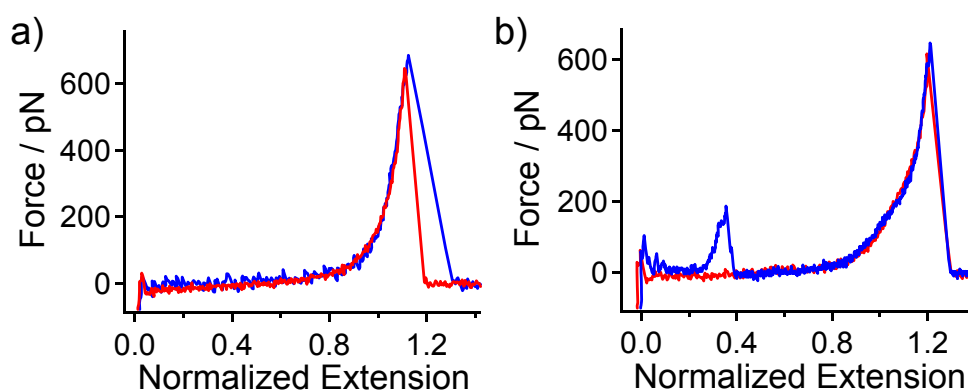


Figure S13. The normalized force curves of PLLA at middle concentration ($100 \mu\text{g}\cdot\text{mL}^{-1}$) obtained in TCE. There are two types of force curves in this case. a) One type of force curve (blue line) is similar to that of PLLA at a low concentration ($3 \mu\text{g}\cdot\text{mL}^{-1}$, red curve) obtained in TCE. b) Another type of force curve (red line) is superposed very well with that of PLLA at a high concentration ($1000 \mu\text{g}\cdot\text{mL}^{-1}$, blue curve) obtained in TCE.

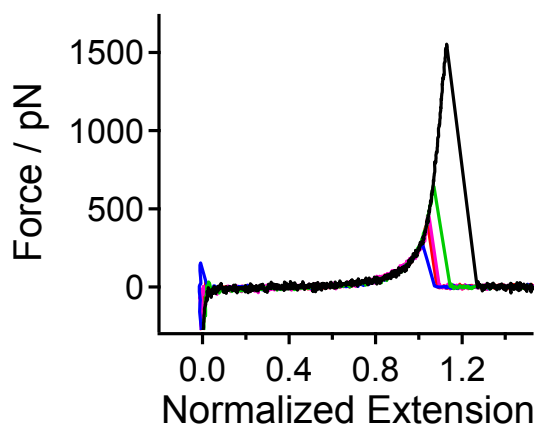


Figure S14. The comparison between the normalized force curves of PDLLA ($1000 \mu\text{g}\cdot\text{mL}^{-1}$) obtained in TCE and the force curve of PLLA (black line, $< 30 \mu\text{g}\cdot\text{mL}^{-1}$) obtained in octylbenzene.

References

- (1) Cui, S.; Yu, J.; Kuehner, F.; Schulten, K.; Gaub, H. E. Double-stranded DNA dissociates into single strands when dragged into a poor solvent. *J. Am. Chem. Soc.* **2007**, *129* (47), 14710-14716.
- (2) Cheng, B.; Cui, S. Supramolecular Chemistry and Mechanochemistry of Macromolecules: Recent Advances by Single-Molecule Force Spectroscopy. *Top. Curr. Chem.* **2015**, *369*, 97-134.
- (3) Auras, R. A.; Lim, L.-T.; Selke, S. E.; Tsuji, H. in *Poly (lactic acid): synthesis, structures, properties, processing, and applications*. John Wiley & Sons: **2011**; Vol. 10.
- (4) Perego, G.; Cella, G. D.; Bastioli, C. Effect of molecular weight and crystallinity on poly (lactic acid) mechanical properties. *J. Appl. Polym. Sci.* **1996**, *59* (1), 37-43.

- (5) Grandbois, M.; Beyer, M.; Rief, M.; Clausen-Schaumann, H.; Gaub, H. E. How strong is a covalent bond? *Science* **1999**, *283* (5408), 1727-1730.
- (6) Sasaki, S.; Asakura, T. Helix distortion and crystal structure of the α -form of poly (l-lactide). *Macromolecules* **2003**, *36* (22), 8385-8390.
- (7) Cui, S.; Yu, Y.; Lin, Z. Modeling single chain elasticity of single-stranded DNA: A comparison of three models. *Polymer* **2009**, *50* (3), 930-935.